

Use of regression analysis for the construction of empirical fragility curves

I. Ioannou & T. Rossetto
University College London, UK

D.N. Grant
Arup, London



15 WCEE
LISBOA 2012

SUMMARY:

The effectiveness of any project aimed at mitigating the consequences of possible future earthquakes on the built environment depends on the accurate quantification of seismic risk. A key component for this is the reliable assessment of structural fragility and in particular the regression analyses commonly adopted for the construction of empirical fragility curves from post-earthquake data. The generalised linear models were found to be theoretically more suitable for the construction of the fragility curves. Nonetheless, the poor fit of the selected regression model, fitted by the latter approach to Italian field stone masonry data, demonstrated the vital role of the diagnostics and the need to increase the complexity of the regression models perhaps by adding more predictor variables, building generalised linear mixed models as well as the need for accurate quantification of the epistemic uncertainty.

Keywords: Empirical fragility assessment, regression analysis, least squares, generalised linear models, local polynomial.

1. INTRODUCTION

Empirical fragility assessment aims at predicting the damage for specific levels of ground motion intensity by constructing a relationship between post-earthquake damage data for various typologies of structures located in a number of affected areas and their corresponding ground motion intensities. These relationships are commonly expressed as fragility curves, which represent the probability that a class of structures reaches or exceeds a level of damage for specified levels of ground motion intensity. Such empirical curves have been mostly constructed by regression analyses (e.g. Rota et al, 2008; Rossetto and Elnashai, 2003). Different regression techniques have been proposed in the fragility literature typically without a thorough discussion on their limitations and their impact on the reliability of the resulting curves. This study discusses the most popular regression analyses procedures, namely the least squares and the maximum likelihood regression, adopted in the empirical fragility assessment literature. The most promising methods are then appraised by constructing empirical fragility curves based on the 1980 Irpinia damage data collected for field stone masonry buildings found in the Cambridge Earthquake Impact Database (1989). The regression analyses are performed using a code written in R (Ihaka and Gentleman, 1996) and Matlab. The Bayesian regression analysis (Straud and Der Kiureghian, 2008) and a few general optimisation techniques found in the empirical fragility assessment literature (e.g. Spence et al, 1992; Jaiswal and Wald, 2011) are not the subject of this paper.

2. EMPIRICAL FRAGILITY ASSESSMENT

In the aftermath of a strong earthquake event, field surveys are often compiled, reporting information for individual structural units or aggregated data associated with groups of structures located in specified areas, termed survey units. These data regard the level of damage of the examined structures, their structural typology and the level of ground motion intensity in the area where they are located. Empirical fragility assessments depend on the quantity and quality of the field damage data and the accuracy of the determined intensity levels. Figure 2.1 depicts common sources of uncertainty associated with the aforementioned components. The uncertainties are separated according to whether they are inherent in the adopted procedure (termed aleatory), or they can, theoretically at least, be reduced by further additional data (termed epistemic). The regression analysis constructs the fragility curves by effectively estimating the parameters of a model which correlates a predictor variable, i.e. the ground motion intensity (*IM*) with a response variable, e.g. the damage, typically expressed in terms of a discrete damage scale (*DS*). The literature so far has been in favour of parametric regression models. Recently, Noh et al (2011) promoted the more flexible nonparametric models which perhaps describe the trend in the damage data better. The following discussion on available regression techniques is based on two assumptions typically found in the empirical fragility literature, although their violation could lead to biased regression parameters and therefore unreliable fragility curves:

- i. *The observations are equally reliable*, i.e. the epistemic uncertainty associated with the observations are considered negligible (see Figure 2.1). This assumption can be met if the data are obtained from a single reliable survey compiled in the aftermath of a strong event.
- ii. *The values of intensity are measured without error*, i.e. the aleatory and epistemic uncertainty associated with the intensity (see Figure 2.1) is ignored. This assumption is typically not met due to the levels of intensity mostly being estimated from ground motion prediction equations (GMPEs). Rota et al (2008) noted that the impact of this uncertainty can be notable but not substantial for the mean fragility curve, however more research is required to estimate the impact on the prediction intervals of the fragility curves.

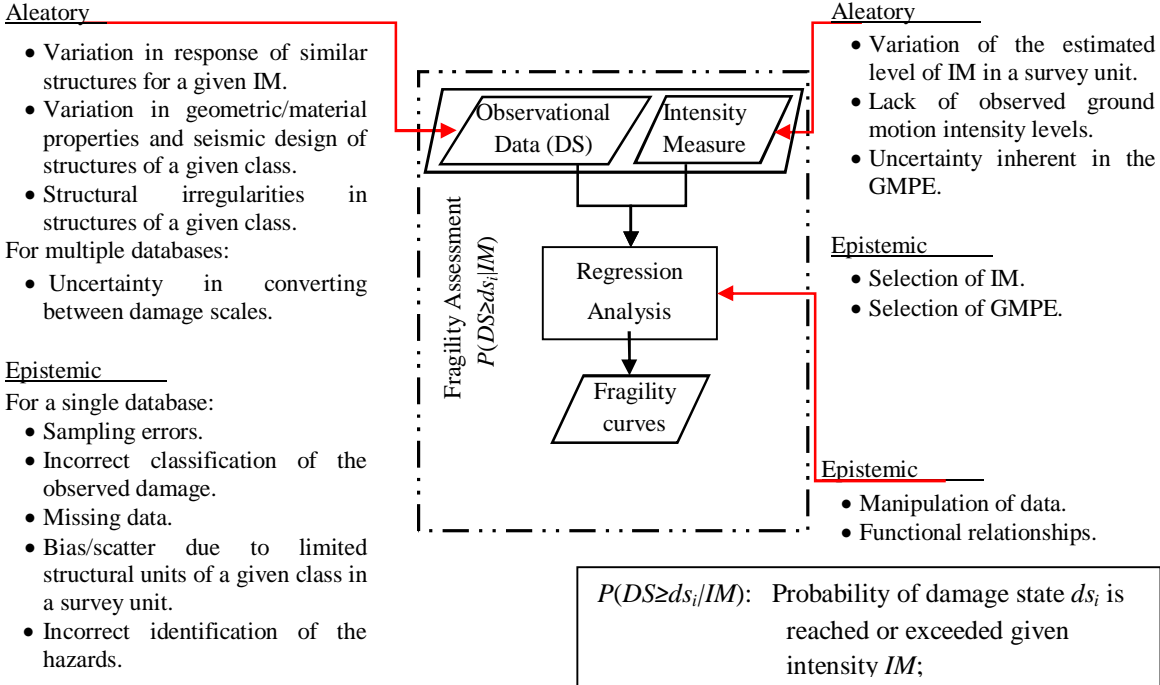


Figure 2.1. Sources of uncertainty in the empirical fragility assessment.

3. REGRESSION ANALYSIS TECHNIQUES

3.1. Parametric Regression Analysis

3.1.1. Existing models for fragility curves

Existing empirical fragility curves have mainly been constructed using the regression models depicted in Table 3.1. The lognormal cumulative distribution function (Eq.(3.1)) is most commonly used as the regression model. Its popularity can be attributed to its three properties. Firstly, this function is constrained in the y-axis between (0, 1) which is ideal for fitting data points expressing aggregated probabilities. With regard to the x-axis, the values are constrained in (0, $+\infty$). This agrees with the range of almost all ground motion intensity measures. Finally, this distribution appears to be skewed to the left, and thus it can, theoretically at least, provide a better estimate for the smaller intensities, where the majority of the data typically lies. The normal cumulative distribution function (Eq.(3.2)) and the logistic distribution (Eq.(3.3)) can be used in cases where the intensity measure can take negative values. Nonetheless, Yamaguchi and Yamazaki (2000) express their fragility curves in terms of this distribution despite their intensity measure being discrete and positive. Similarly, Basöz et al (1999) and O' Rourke and So (2000) used the Eq.(3.3), whose fit is close to Eq.(3.2), for performing logistic regression. Instead of the aforementioned two cumulative probability distributions, an exponential function expressed by Eq.(3.4), unconstrained in both x- and y-axis has also been adopted by Rossetto and Elnashai (2003) and Amiri et al (2007). The use of a non-probability distribution function to express the fragility curves may have implications in the risk assessment which requires its coupling with a hazard curve to produce the annual probability of reaching or exceeding a damage state.

Table 3.1. Regression models and their parameters used in the literature to express the fragility curves.

Eq.:	$P(DS \geq ds_i IM = x)$	Parameters:	References
(3.1)	$\Phi\left(\frac{\ln(x) - \lambda}{\zeta}\right)$	μ, ζ	e.g. Yamaguchi and Murao, 2000; Shinozuka et al, 2000; Sarabandi et al, 2004; Rota et al, 2008; Liel and Lynch, 2009
(3.2)	$\Phi\left(\frac{x - \mu}{\sigma}\right)$	μ, σ	Yamaguchi and Yamazaki, 2000.
(3.3)	$\frac{1}{1 + \exp(-(\theta_0 + \theta_1 x))}$	θ_0, θ_1	Basöz et al, 1999; O' Rourke and So, 2000
(3.4)	$1 - \exp(-\theta_0 x^{\theta_1})$	θ_0, θ_1	Rossetto and Elnashai, 2003; Amiri et al, 2007

3.1.2. Procedures for estimating the unknown parameters of the regression models

Recent studies (Rossetto and Elnashai, 2003; Amiri et al, 2007; Rota et al, 2008) constructed empirical fragility curves for buildings by nonlinear least squares regression. According to this approach, the response variable is expressed in terms of the probability of a damage state, ds_i , being reached or exceeded. The predictor variable is expressed in terms of the ground motion intensity. The relationship between the continuous predicted and predictor variables is written as:

$$y_j = m(x) + \varepsilon_j = P(DS \geq ds_i | x_j) + \varepsilon_j \quad (3.4)$$

where y_j is the empirical frequency of reaching or exceeding ds_i for the buildings of bin j obtained by grouping the post-earthquake damage data in bins of similar ground motion intensities; $m(\cdot)$ is the regression model; $P(DS \geq ds_i | x_j)$ is the mean fragility curve, expressing the probability that ds_i is reached or exceeded given intensity x_j ; ε_j is the error between the predicted and observed value of the response variable. The least squares method was used in order to estimate the optimum regression parameters of the selected model by:

$$\theta^{opt} = \arg \min \sum_{j=1}^M (\varepsilon_j)^2 = \arg \min \sum_{j=1}^M w_j (y_j - m(x))^2 \quad (3.5)$$

where w_j is a weight for the bin j . Eq.(3.5) was solved numerically by the aforementioned studies aiming mainly, but not exclusively, at fitting Eq.(3.3) to post-earthquake damage data (Rossetto and Elanshai, 2003; Amiri et al, 2007). Nonetheless, this approach is based on the following assumption:

- i. *The errors ε_j are independently and normally distributed in all bins with mean zero and constant standard deviation.*

These studies have not explicitly assessed the validity of this assumption, perhaps due to their main focus on the mean fragility curve, which is not affected by its violation. Nonetheless, the fragility curves are bounded in (0,1) in the y-axis, which may violate the normal distribution of errors for extreme level of intensity. In addition, for extreme levels of intensity, the uncertainty in the response variable (e.g. the probability of collapse) is very small and increases for intermediate levels of intensity. Thus, the error cannot be constant for every level of uncertainty. The violation of this assumption produces biased estimates of the standard error leading to unreliable prediction intervals.

A closed form solution of Eq.(3.5) was adopted by the majority of the studies which correlated damage data with a measure of ground motion intensity (i.e. Yamazaki and Murao, 2000, Yamaguchi and Yamazaki, 2001; Liel and Lynch, 2009). With the exception of Rota et al (2008), this linear least squares method is adopted for the determination of the parameters of the two cumulative probability distributions expressed by Eq.(3.1) and Eq.(3.2) (see Table 3.1). This requires the linearization of Eq.(3.4) through the transformation of the field data into the form: $(\ln(x_j), \Phi^{-1}(y_j))$ or $(x_j, \Phi^{-1}(y_j))$, respectively. Although, this approach does not suffer from the limitations of the nonlinear least squares technique, its applicability is limited due to the unfeasibility of the transformation for extreme values of y_j (0 and 1). Procedures (e.g. Porter et al, 2007) that attempted to deal with the transformation of $y_j=0$ seem questionable.

By contrast, the studies focused on the construction of empirical fragility curves for bridges (e.g. Basöz et al, 1999; Shinozuka et al, 2000) and steel tanks (O' Rourke and So, 2000) constructed individual fragility curves by expressing the response variable in terms of a binary response y_j for each building j :

$$y_j = \begin{cases} 0 & DS < ds_i \\ 1 & DS \geq ds_i \end{cases} \quad (3.6)$$

Alternatively the response variable expressed the y_j counts of data with $DS < ds_i$ and $DS \geq ds_i$ for bin j with intensity x_j . The parameters of the fragility curves are then obtained by maximising the distribution of the damage data, which is considered binomial:

$$\boldsymbol{\theta}^{opt} = \arg \max L(\boldsymbol{\theta}) = \arg \max \log \left\{ \prod_{j=1}^M \left[\binom{m_j}{y_j} P(DS \geq ds_i | x_j; \boldsymbol{\theta})^{y_j} [1 - P(DS \geq ds_i | x_j; \boldsymbol{\theta})]^{m_j - y_j} \right] \right\} \quad (3.7)$$

where M is the total number of structural units or the number of bins in the database. Contrary to the nonlinear least squares regression, this approach recognises that the fragility curves are probability distributions. Shinozuka et al (2000) used a maximum likelihood algorithm in order to estimate the two parameters of the lognormal CDF from Eq.(3.7). Basöz et al (1999) and O'Rourke and So (2000) constructed generalised linear models and estimated the regression parameters from Eq.(3.7) through a weighted iterative least squares technique. The use of generalised linear models is also adopted in this study due to their ability to use different functions to express fragility curves and to add more predictor variables in order to improve the model.

Despite the advantages of the independent construction of each fragility curves using Eq.(3.7), the possible overlapping of these curves, which leads to meaningless results, cannot be prevented. This can be avoided by performing ordinal regression (see Shinozuka et al, 2000) analysis, which

recognises the ordered categorical nature of the damage data.

3.2. Nonparametric Regression Analysis

3.2.1. Local polynomial regression

Local polynomial regression is effectively a weighted moving average technique aimed at the estimation of a nonparametric relationship, expressed by Eq.(3.4), between the continuous predicted variable expressing the probability of a level of damage being reached or exceeded and the predictor variable IM . The determination of this relationship is achieved by applying the weighted least squares method locally at data points as:

$$\theta^{opt}(x) = \arg \min \sum_{j=1}^M (\varepsilon_j)^2 = \arg \min \sum_{j=1}^M K(x_j - x; h) (y_j - m(x_j - x; \theta(x)))^2 \quad (3.8)$$

where M is the number of data points, y_j is the empirical frequency of reaching or exceeding ds_i for the buildings in bin j obtained by grouping the damage data in bins of similar ground motion intensities, $m(\cdot)$ is the locally fitted polynomial of N degree, here expressing the fragility curve; $K(\cdot)$ is the weighting component of an bin j , termed kernel; h is a smoothing parameter termed bandwidth which is widely accepted to be the most important parameter. This technique depends on the assumptions outlined in section 3.1.2 regarding the distribution of the error and therefore (Bowman and Azzalini, 1997):

- i. There is no guarantee that the obtained nonparametric curve lies between 0 and 1.
- ii. The assumption regarding the error (see section 3.1.1) is most likely to be violated.

In the fragility literature, Noh et al (2011) adopt this approach to construct analytical fragility curves using a zero degree polynomial, termed the Nadaraya-Watson (1964) kernel estimator which seemed to overcome the aforementioned limitations.

3.2.1 Local likelihood regression

The limitations of the local polynomials can also be overcome with the local likelihood regression, which essentially extends the local averaging procedures to the generalised linear models. According to this approach, the likelihood function of the model is weighted by a kernel function in the form:

$$\theta^{opt}(x) = \arg \max \left[\sum_{j=1}^M K(x_j - x; h) L_j(\theta(x)) \right] \quad (3.9)$$

This method is capable of treating binary damage data (see Eq.(3.6)) for individual structural units. Despite the advantages over the local polynomial methods, it has not been applied for the fragility assessment of structures. In what follows this method is compared to the parametric generalised linear models.

4. CASE STUDY

From the study of the literature, the parametric generalised linear models and the local likelihood regression technique were found to be the most appropriate for the empirical fragility assessment. These techniques are appraised here by the construction of fragility curves using post-earthquake data collected from 16,759 field stone masonry buildings, located in Campania and Basilicata (southern Apennines, Italy) which were affected by the 1980 Irpinia earthquake. This event is the strongest recorded earthquake in Italy and its database, found in the Martin Centre Earthquake Vulnerability Database (1989), is considered well-recorded and is frequently used for empirical fragility assessment (Braga et al, 1982; Sabetta et al, 1998; Roca et al, 2006; Rota et al, 2008).

4.1. Intensity measure

The assessment of the impact of the 1980 Irpinia earthquake event on the buildings in the surveyed municipalities requires the selection of one or more ground motion intensity measures as well as the determination of their levels at the 41 municipalities. The level of intensity over each municipality is assumed to be constant, in line with most existing studies. This assumption is considered reasonable here due to the small area covered by each municipality (on average 24km²).

4.1.1. Selection and evaluation of IM

The ground motion intensity is measured in terms of peak ground acceleration (PGA), which has been the most widely adopted continuous intensity measure in the empirical vulnerability/fragility assessment literature. Other measures will be investigated in future studies. The levels of PGA (in m/s²) in the examined municipalities have been obtained from the Cambridge Earthquake Impact database. These latter values were based on the USGS ShakeMap.

4.2. Data description

The 1980 Irpinia database was constructed by the one-stage cluster sampling method (Levy and Lemeshow, 2008); i.e. the total number of buildings from 41 municipalities (out of more than 600 affected by the event) in the Campania-Basilicata area was surveyed (Braga et al, 1982). The largest building class in this database consists of field stone masonry building and is adopted here for the demonstration of the regression techniques. The number of field stone masonry buildings surveyed in each municipality varied widely from 3 to 1573. The observed damage was classified in six discrete states (no damage-collapse) according to MSK-76. Figure 4.1b highlights the significant (~25%) percentage of buildings which suffered heavy damage or collapse. This can be attributed to the sample being dominated by the field stone masonry buildings with wooden floors (see Figure 4.1a), which are the most vulnerable of the four different types of horizontal structural system noted in the database.

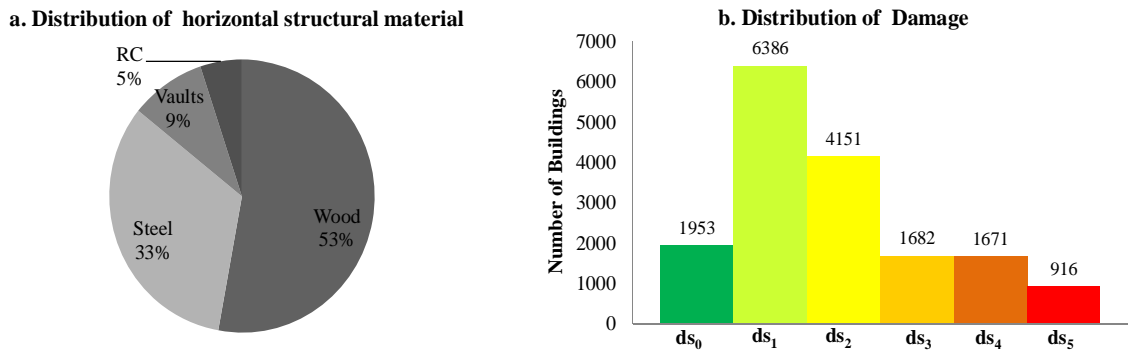


Figure 4.1. Frequency of a. the four types of the horizontal structural material b. the 6 states of the observed damage in the population of field stone masonry buildings.

4.2. Results

The parametric and nonparametric generalized linear models are fitted to the 1980 Irpinia damage data by numerically solving Eq.(3.7) and Eq.(3.9), respectively and compared to the nonlinear least squares approach (Eq.(3.5)). The parametric model is adopted in order to fit the commonly used lognormal distribution to the 41 data points (x_j, y_j) , expressing the counts of buildings that suffered damage $DS < ds_i$ and $DS \geq ds_i$ for each municipality j and the corresponding intensity x_i . The estimation of the regression parameters is achieved by a probit link function in the form:

$$\Phi^{-1}\left(P\left(DS \geq ds_i \mid PGA = x_j\right)\right) = \theta_0 + \theta_1 \ln\left(x_j\right) \quad (4.1)$$

This approach is preferred to its equivalent building-by-building approach due to its more helpful tools for assessing the fit of the model and it is based on the assumption that the buildings are independent. A building-by-building approach is used in order to fit a nonparametric curve using the local

likelihood regression with bandwidth $h=0.5$ to the 16,579 data points. The bandwidth is selected by trial and error which avoided the very large values, whose fit was unable to capture any trend in the data as well as the small values, whose fit was influenced by the few points with large intensities. The regression model expressed by Eq.(3.4) was also used in order to fit lognormal curves to 41 data points (x_j, y_j) expressed as the empirical frequency, y_j , of a group of buildings, located in municipality j with intensity x_j , reaching or exceeding ds_i . The latter fragility curves were fitted by the nonlinear least squares technique, based on the Gauss-Newton algorithm. The mean fragility curves constructed by the three aforementioned models for the five MSK-76 damage states are depicted in Figure 4.2.a,b,c. For each ds_i , the over-dispersed nonparametric fragility curves show no real advantage in describing the trend in the data by being close to their parametric counterpart. Therefore, in what follows the focus is on the more powerful parametric generalised linear model. It can also be noted that the fragility curves constructed by the latter regression do not overlap for the range of available intensities indicating that the independent construction of fragility curves leads to meaningful results and therefore the ordinal regression is not explored here. These curves also seem to be reasonably close to their counterparts obtained by the nonlinear least square regression, suggesting that for this case study the construction of different regression models is not important for the estimation of the mean fragility curves.

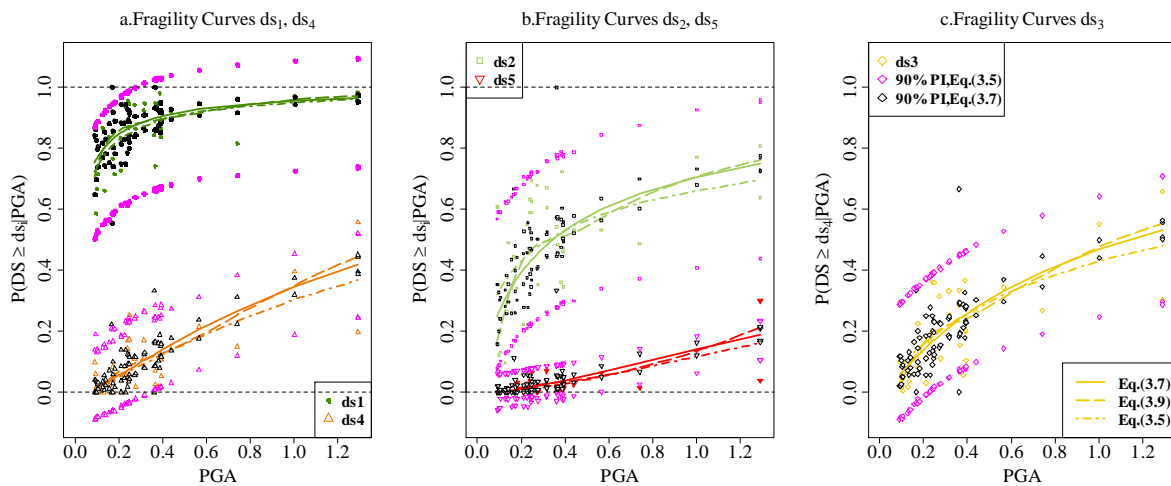


Figure 4.2. Fragility curves and their associated 90% prediction intervals (PI) obtained by parametric (for Eq.(3.7)) and nonparametric (for Eq.(3.5)) bootstrap corresponding to a. $ds_{1,4}$ and b. $ds_{2,5}$ and c. ds_3 .

The effectiveness of the selected model in representing the field data is assessed next. The goodness-of-fit of the generalized linear model is explored by a series of significance tests. Both the likelihood ratio test, which compares the fit of the lognormal distribution with the fit of a model expressed by a constant, and the Wald test highlighted the statistical significance of the PGA for all five fragility curves. An alternative likelihood ratio test, which compares the fit of the lognormal distribution with the fit of a saturated model, i.e. a model whose number of parameters is equal to the number of data points, indicated that the five lognormal distributions are unlikely to have generated their associated data points. The poor fit was also confirmed by the Pearson chi-square significance test. The aforementioned tests do not have the power to indicate ways to improve the model. For this reason, the graphical assessment of the validity of the assumptions is required. The linear relationship of the $\ln(\text{PGA})$ (see Eq.(4.1)) is assessed in Figure 4.3.a for ds_5 by plotting the trend of the partial residuals $(\theta_1 \ln(x_j) + \varepsilon_j)$ against the logarithm of the intensity. The assessment seems to confirm the linearity assumption. Similarly, this assumption is found to be valid for the remaining four curves. The assumption that the Pearson residuals have mean zero and constant variance equal to 1 seems to be violated in Figure 4.3.b for ds_5 where the variance of the residuals appears to be heteroskedastic and three data points, i.e. points 40, 41 corresponding to the highest level of PGA and point 21 corresponding to an unusually high level of collapse, seem to be influential. The sizeable number of residuals outside the interval $[-2,2]$ also confirm the poor fit of the binomial distribution. The homoskedasticity assumption also seems to be grossly violated in the scale-location plots in Figure

4.3.c where the monotonic increase of the standardized Pearson residuals is noted for ds_5 . The steepness of the curve can be, at least partially, attributed to the influential role of the points 40 and 41. Similar trends are noted for cases ds_3 and ds_4 . The trend appears to be considerably flatter for ds_1 and ds_2 , suggesting that the variance of the residuals is constant for these two fits. A departure from the normality is also noted by Q-Q plots for the residuals (see Figure 4.3.d for ds_5). This assumption, however, is weak as it appears to be violated even when the model fits the data) and therefore the QQ plot can be used to confirm the presence of potentially influential points.

The violation of these assumptions can be caused by either systematic deficiencies (e.g. influential points, wrong link function, missing predictor variables) or over-dispersion due to dependencies in the building performance within a given municipality, which is not present between different municipalities. The presence of potential influential points is reinforced by the plot of the Cook's distance (i.e. measures the effect on the fitted values of removing a specified data point) in Figure 4.3.e. A similar procedure identified potential influential points, not necessarily the same as ds_5 , for the lognormal fit corresponding to the remaining four damage states. However, Figure 4.3.f shows that the removal of these points (in black) yields negligible differences in the fragility curves, with the exception of the case ds_2 and ds_5 where the difference in the fit is notable. Given that the removal of these points in the latter two cases from the sample is not justifiable, a robust logistic regression could potentially provide an improved fit which is not influenced by such points. Other available link functions, apart from the adopted normal distribution, were selected such as the logit, the log and the complementary log-log. The fit of the new model was not improved. This indicates that perhaps important predictor variables are missing from Eq.(4.1). These ignored variables include dummy variables which account for the different levels of vulnerability of the data or variables associated with the hazard such as the soil conditions or the source-to-site distance. The latter, however, is an indication of insufficient ground motion intensity measure and the selection of a different measure should be tested. Last but not least, the poor fit of the model could perhaps be improved by the construction of generalised linear mixed models which incorporate the dependence in the damage data located in each municipality (see Straub and Der Kiureghian, 2008). More research is underway for trying to quantify this uncertainty in each municipality given the poor quality of the aggregated data.

Table 4.1. Diagnostics for the maximum likelihood and nonlinear least squares regression techniques for fitting Eq.(3.1).

Tests/ DS	Maximum Likelihood					Nonlinear Least Squares				
	1	2	3	4	5	1	2	3	4	5
Homoscedasticity	A	A	A	A	R	R	R	A	A	R
Normality	A	A	R	R	R	R	A	A	A	R
R: Non-valid assumption, A: Valid assumption										

With respect to the goodness of fit of the curves constructed by nonlinear least squares regression, their homoscedasticity and normality are explored graphically using plots similar to Figure 4.3 b-c. In line with the discussion in section 3.1.2, the lognormal fit appears to violate the homoscedasticity and, for the extreme cases ds_1 and ds_5 , the normality assumption as well (see Table 4.1). These violations, however, do not affect the fit of the mean curves but the prediction intervals discussed below.

The 90% prediction intervals, i.e. intervals capturing the uncertainty in estimating the true mean as well as the variability in the field data, of the lognormal fragility curves is examined next. The intervals round the curves constructed by generalised linear models and the model expressed by Eq.(3.4) are also generated from parametric and nonparametric bootstrap techniques, respectively (Chandler and Scott, 2011). The point-wise 90% prediction intervals for the five fragility curves are depicted in Figure 4.2 for the two methods. The intervals based on the parametric bootstrap appear to be narrow, under-predicting some data points and over-predicting others. This behaviour is an indication of poor fit highlighting the need for further research in building reliable intervals which can be used for future predictions. It should be mentioned that the points which are well out of bounds correspond to data points, based on less than 20 buildings, which favours existing approaches (e.g.

Karababa and Pomonis, 2010) according to which these data points are removed before the regression analysis. By contrast, the prediction intervals generated by the nonparametric bootstrap around the fragility curves constructed by the least squares regression appear to be wider, with constant width, and systematically over-predicting the observed data points having very large or very small probabilities. This is in line with the violation of the homoscedasticity assumption. Another drawback of these intervals is the failure of the least squares method as well as the bootstrap technique to account for the fitted lognormal distribution being bounded in (0,1) leading to meaningless (<0 or >1) bounds for the fragility curves corresponding to extreme (ds_1 and ds_5) as well as intermediate (ds_3 and ds_4) damage states.

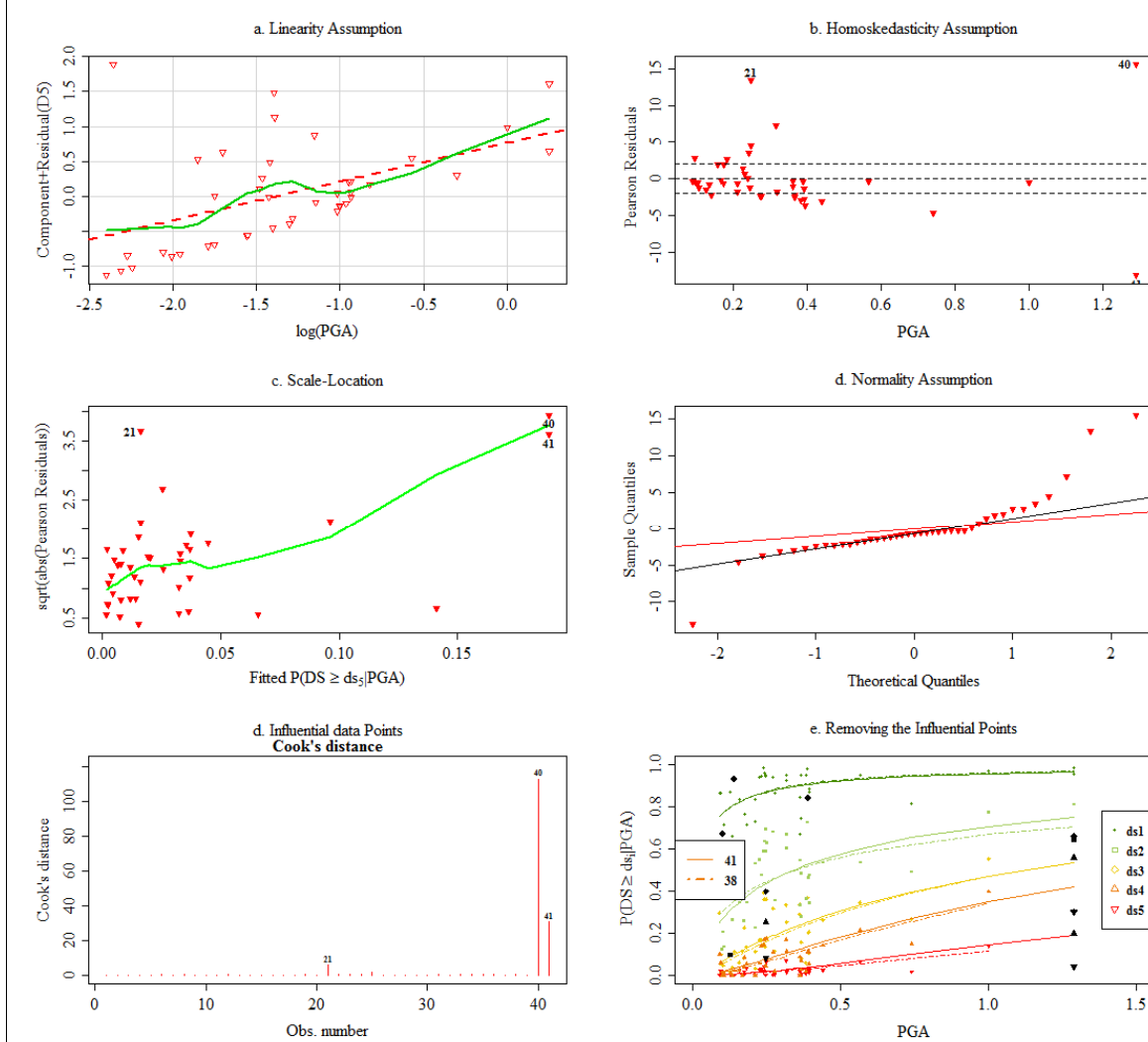


Figure 4.3. a. Test of the linearity assumption, b. test of the homoscedasticity assumption, c. scale-location, d. test of the normality assumption, e. Cook's distance and f. comparison of the fragility curves with (41) and without (38) the influential points.

5. CONCLUSIONS

Overall, it was discussed that empirical fragility curves can be reliably constructed by the use of generalized linear models. Their use for the construction of lognormal fragility curves for field stone masonry buildings emphasized on the diagnostics (mostly ignored in the empirical fragility assessment literature) and the construction of the prediction intervals. The case study highlighted the limitations of the two mostly used regression procedures in modeling the uncertainty as well as areas of future research which can potentially improve the reliability of fragility curves for future predictions. These areas include the use of more advanced regression procedures (e.g. robust regression), the development of more complex models, e.g. generalized linear mixed models with perhaps more

predictor variables, which also account for the uncertainty in the ground motion intensity and of procedures which can reliably represent the epistemic uncertainty.

ACKNOWLEDGEMENT

The authors acknowledge financial support from the Global Earthquake Model (GEM) Project.

REFERENCES

- Amiri G.G., Jalalian M., Amrei S.A.R. (2007). Derivation of vulnerability functions based on observational data for Iran. *Proceedings of International Symposium on Innovation & Sustainability of Structures in Civil Engineering*.
- Basöz N.I., Kiremidjian A.S., King S.A., Law K.H. (1999). Statistical analysis of bridge damage data from the 1994 Northridge, CA, earthquake. *Earthquake Spectra*, **15:1** 25-54.
- Braga F., Dolce M. and Liberatore D. (1982). Southern Italy November 23, 1980 earthquake: a statistical study of damaged buildings and an ensuing review of the M.S.K.-76 scale, Report, Rome, Italy.
- Bowman A.W. and Azzalini A. (1997). Applied smoothing techniques for data analysis. *Oxford Science Publications*.
- Chandler R.E., Scott E.M.. (2011). Statistical methods for trend detection and analysis in the environmental science. *John Wiley & Sons*.
- Ihaka R., Gentleman R. (1996). R: A language for data analysis and graphics. *Journal of Computational and Graphical Statistics* **5:3**, 299-314.
- Karababa F.S., Pomonis A. (2010). Damage data analysis and vulnerability estimation following the August 14, 2003 Lefkada Island, Greece, Earthquake. *Bulletin of Earthquake Engineering*, **9:4**, 1015-1046.
- Levy P.S., Lemeshow S. (2008)..4th ed., John Wiley & Sons.
- Liel A.B., Lynch K.P. (2009) Vulnerability of reinforced concrete frame buildings and their occupants in the 2009 L'Aquila. *Natural Hazards Review* (in press).
- Noh H. Y., Lignos D.G., Nair K. and Kiremidjian A. (2011). Development of fragility functions as a damage classification/prediction method for steel moment-resisting frames using a wavelet-based damage sensitive feature. *Earthquake Engineering & Structural Dynamics* **41:4**,681-696.
- Jaiswal K., Wald D., D'Ayala D. (2011). Developing empirical collapse fragility functions for Global building types. *Earthquake Spectra*, in press [accepted on June 15, 2010].
- Orsini G. (1999). A model for buildings' vulnerability assessment using the parameterless scale of seismic intensity (PSI). *Earthquake Spectra*, **15:3**, 463-483.
- O'Rourke M.J., So P. (2000). Seismic fragility curves for on-grade steel tanks. *Earthquake Spectra* **16:4** 801-815.
- Roca A., Goula X., Susagna T., Chávez J., González M. and Reinoso E. (2006). A simplified method for vulnerability assessment of dwelling buildings and estimation of damage scenarios in Catalonia, Spain. *Bulletin of Earthquake Engineering* **4:2**, 141-158.
- Porter K., Kennedy R., Bachman R. (2007). Creating fragility functions for performance-based earthquake engineering. *Earthquake Spectra* **23:2**, 471-489.
- Rossetto T. and Elnashai A. (2003). Derivation of vulnerability functions for European-type RC structures based on observational data. *Engineering Structures* **25:10**, 1241-1263.
- Rota M., Penna A. and Strobbia C.L. (2008). Processing Italian damage data to derive typological fragility curves. *Soil Dynamics and Earthquake Engineering* **28:10-11**, 933-947.
- Sabetta F., Goretti A. and Lucantoni A. (1998). Empirical fragility curves from damage surveys and estimated strong ground motion. *Proceedings of 11th European Conference on Earthquake Engineering*.
- Shinozuka M., Feng M.Q., Lee J., Naganuma T. (2000). Statistical analysis of fragility curves. *Journal of Engineering Mechanics*, **126:12** 1224-1231.
- Spence R.J.S., Coburn A.W., Pomonis A. (1992). Correlation of ground motion with building damage: The definition of a new damage-based seismic intensity scale. *Proceedings of 10th World Conference on Earthquake Engineering*.
- Straud D. and Der Kiureghian A. (2008). Improved seismic fragility modelling from empirical data. *Structural Safety*, **30:4** 320-336.
- Yamaguchi N., Yamazaki F. (2001). Estimation of strong motion distribution in the 1995 Kobe earthquake based on building damage data. *Earthquake Engineering and Structural Dynamics*, **30:6** 787-801.
- Yamazaki F., Murao O. (2000). Vulnerability functions for Japanese buildings based on damage data due to the 1995 Kobe earthquake. *Implication of Recent Earthquakes on Seismic Risk, Series on Innovation and Construction, Imperial College Press 2, London, UK*.